GEOG 321 - Reading Package Lecture 27

T. R. Oke (1987): 'Boundary Layer Climates', 2nd Edition
Pages 158 - 167

5

Climates of non-uniform terrain

In the preceding sections we have considered the energy and water balances of a range of relatively simple surfaces. The balance relationships we have been able to use have assumed that the surface in question is extensive and flat, and is virtually uniform in character (ideally it is an infinite homogeneous plane). If this is so, then the response of the surface to the energy and mass exchanges is everywhere equal. This means that all gradients of climatological properties will be perpendicular to the active surface, and all fluxes are in the vertical direction.

In the real world relatively few surfaces are flat, few could be considered homogeneous, and none are infinite. On the contrary the Earth's surface is a patchwork quilt of different surface slopes and materials. The scale of the units composing this quilt extends all the way from the oceans and continents down to individual leaves and even smaller. As an example consider the case of a group of agricultural fields, some ploughed and bare, some fallow, some in crops. Each of these fields possesses its own combination of radiative, thermal, moisture and aerodynamic properties, such as albedo, soil conductivity, soil moisture, surface roughness, etc. Each field therefore will tend to regulate and partition the available energy and water in a different manner, giving each a unique energy and water balance. These differences will be manifested as different surface, sub-surface and atmospheric climates in terms of temperature, humidity, and wind speed profiles. Thus there will be spatial discontinuity of climates, and horizontal gradients will exist. Near the surface at the boundaries between the fields these gradients will be greatest, and horizontal interactions will occur.

The climatic response of the above array of fields would be further complicated if they were situated in an area of varied topography. Solar loading differences would arise because of differences of slope and aspect, moisture availability would vary because of areal precipitation and drainage characteristics, and the wind field would be affected by channelling and shelter effects. One of the greatest challenges in modern atmospheric science is to understand the way in which these interactions take place. Only then

will we be able to approach a fully dimensional climatology which accounts for the space and time domains.

In our further study of the climates of non-uniform terrain it is convenient to deal first with the effects of spatial variation in surface character, and second with the effects of topography.

1 EFFECTS OF SPATIAL INHOMOGENEITY

Two different cases will be considered: first, we will note the modification of atmospheric properties as air, already in horizontal motion, moves from one distinct surface type to a different one—these are *advective effects;* second, we will consider the circulation of air induced by contrasting surface properties when regional winds are weak—these are *thermal circulation systems*.

(a) Advective effects

Three different advective effects are generally recognized: the *'clothesline effect',* the *'leading-edge or fetch effect',* and the *'oasis effect'*.

(i) 'Clothesline effect'

This effect is normally restricted to the flow of air *through* a vegetative canopy. The ideal conditions exist at a vegetative stand border, as for example at the edge of a crop surrounded by warmer, drier ground; or at the edge of a forest bordered by fields. The situation is well illustrated by the horizontal flow (ΔQ_A) depicted in Figure 4.1a. If the air entering the crop from the right is warm and dry it will increase both the heat supply, and the vapour pressure gradient between the transpiring leaves and the crop air. The net result is to enhance the evaporation rate and hence to more rapidly deplete the soil moisture close to the stand border. Further into the crop the air cools down and acquires moisture, thus causing it to adjust to the more typical conditions within the stand.

At the edge of crops the soil moisture depletion, crop desiccation, greater wind buffeting, and greater exposure to new plant pests and disease commonly combine to stunt crop growth for a few metres in from the border.

(ii) 'Leading-edge or fetch effect'

As air passes from one surface-type to a new and climatically different surface, it must adjust to a new set of boundary conditions. As shown in Figure 5.1 the line of discontinuity is called the *leading-edge*. The adjustment is not immediate throughout the depth of the air layer, it is generated at the
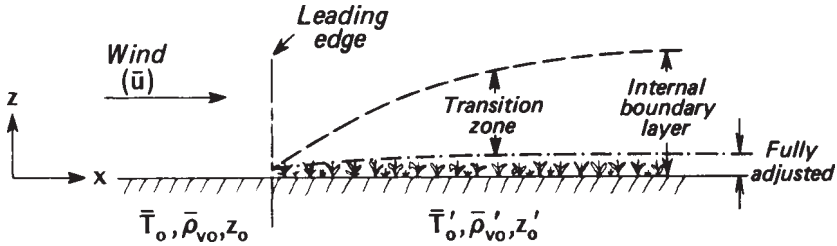
Figure 5.1 The development of an internal boundary layer as air flows from a smooth, hot, dry, bare soil surface (with surface values $\overline{T}'_0$, $\overline{\rho}'_{v0}$, z'_0) to a rougher, cooler and more moist vegetation surface (with new surface values $\overline{T}'_0$, $\overline{\rho}'_{v0}$, z'_0).

surface and diffuses upward. The layer of air whose properties have been affected by the new surface is referred to as an *internal boundary layer,* and its depth grows with increasing distance, or *fetch,* downwind from the leading-edge. It is only in the lower 10% of this layer that the conditions are fully adjusted to the properties of the new surface. The remainder of the layer is a transition zone wherein the air is modified by the new surface but is not adjusted to it. The properties of the air above the internal boundary layer remain determined by upwind influences and not those of the surface immediately beneath.

To illustrate the manner in which adjustment takes place consider the case of air flowing from a dry bare soil surface to a fully moist low vegetation cover. From our previous discussion of the climates of these two surface-type (Chapters 3 and 4) we may anticipate that on a summer day the air has to adjust from a relatively smooth, hot and dry surface to one which is rougher, cooler and wetter. Initially we will restrict consideration to moisture changes in the new internal boundary layer. If we assume there is no major across-wind exchange (called the y direction) then we may conveniently analyse the vertical and along-wind (z and x directions respectively) in terms of the two-dimensional 'boxes' shown in Figure 5.2a. Air with a vapour content $\overline{\rho}_v^\dagger$ (kg m^{-3}) moves from the dry to the wet surface at a speed $u^\dagger$ (m s^{-1}). Hence the rate of horizontal moisture transport, A (kg m^{-2} s^{-1}) is:

$$A = u\rho_v \tag{5.1}$$

In Figure 5.2a the vertical fluxes of water vapour into and out of the boxes are shown by vector arrows the lengths of which are proportional to the strength of the flux. The vertical arrows represent the evaporation fluxes, and the horizontal arrows the advective fluxes. We will assume no net

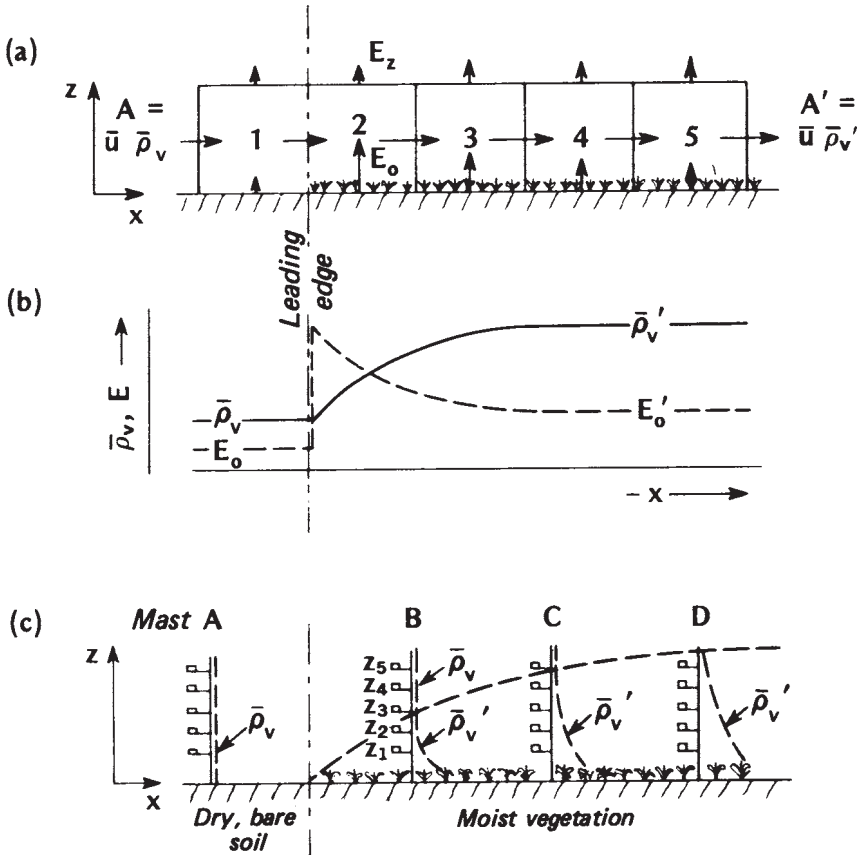† Averaged quantity over the depth of the layer.

Figure 5.2 Moisture advection from a dry to a wet surface, (a) Evaporation rates and the vapour balance of a surface air layer (fluxes of vapour are proportional to the length of the arrows), (b) Surface evaporation rate (E_0), and mean water vapour concentration of the air layer, (c) Vertical profile of water vapour in relation to the developing boundary layer.

condensation or evaporation of vapour *within* the boxes. Hence assuming conservation of vapour the sum of the lengths of the input arrows equals that of the output arrows. If the vertical arrows are of different lengths this indicates divergence or convergence of the vertical flux (Figures 2.1a, b, p. 35) and a non-constant flux layer. If the horizontal arrows are dissimilar it indicates divergence or convergence of the horizontal flux (Figure 2.1c) and that advection is in operation, and the *difference* in their length is a measure of the net moisture advection (ΔA). If total input does not match output that box experiences a change in average humidity.

The vapour flow over the 'dry' upwind surface (box 1 in Figure 5.2a) is essentially non-advective. The horizontal arrows are equal and small, and

the vertical arrows are similarly in balance (i.e. evaporation at the surface, E_0 equals that passing through the reference level z at the top of the box, E_z). As the air crosses the leading-edge into box 2 the surface evaporation rate rises sharply because there is an extremely strong gradient in vapour concentration between the moist surface and the 'dry' air. This increase cannot immediately spread upward, so E_0 exceeds E_z and there is an increase of vapour in the box (Figure 5.2b), and hence a larger horizontal transport out of the downwind side of box 2 (Figure 5.2a).

This process continues in boxes 3 and 4 but because of the accumulation of vapour with distance the surface-to-air vapour gradient weakens and with it the surface evaporation input. Finally at box 5 a new equilibrium situation arises where the mean content reaches a value which is more typical of the moist surface, and which does not overstimulate the surface evaporation regime. Downwind of box 5 both the horizontal and vertical fluxes are constant with distance and the air layer has become fully adjusted to the properties of the new surface.

The corresponding adjustment of the vertical profile of water vapour is given in Figure 5.2c. The upwind profile is very weak as befits a dry surface. The increased vapour content occurs first near the surface, which is the vapour source, and is diffused upwards to affect a deeper layer with increasing distance downwind.

The height of the fully adjusted boundary layer can be viewed as the level at which the vertical vapour flux equals the local surface value. This layer has been found to grow rather slowly requiring a fetch distance of 100 to 300 m for every 1 metre increase in the vertical. It is important to take account of this when setting-up instrumentation masts. For example in Figure 5.2c the levels z_4 and z_5 at mast B should not be used if the data are intended to characterize the conditions of the vegetated surface. The depth of the total internal boundary layer develops much more rapidly, commonly requiring a fetch of from 10 to 30 m for every 1 metre increase in the vertical, but the rate depends on the relative change of roughness between the two surfaces and the state of atmospheric stability. For example the rate will be greater if air moves from a smooth to a much rougher surface during unstable conditions because turbulence would be well developed and able to diffuse properties easily.

In addition to moisture changes the contrast of surface temperature and roughness between the bare soil and vegetated surfaces would give rise to adjustments in the sensible heat flux and momentum exchange downwind of the discontinuity, and these would in turn influence the mean air temperature and wind speed. The anticipated form of these changes are shown in Figure 5.3. The increased evaporative cooling of the vegetated surface would considerably reduce the value of the surface heat flux compared with that upwind. In fact the cooling may produce a surface-based inversion (Figure 5.3c). This means that the sensible heat flux will be
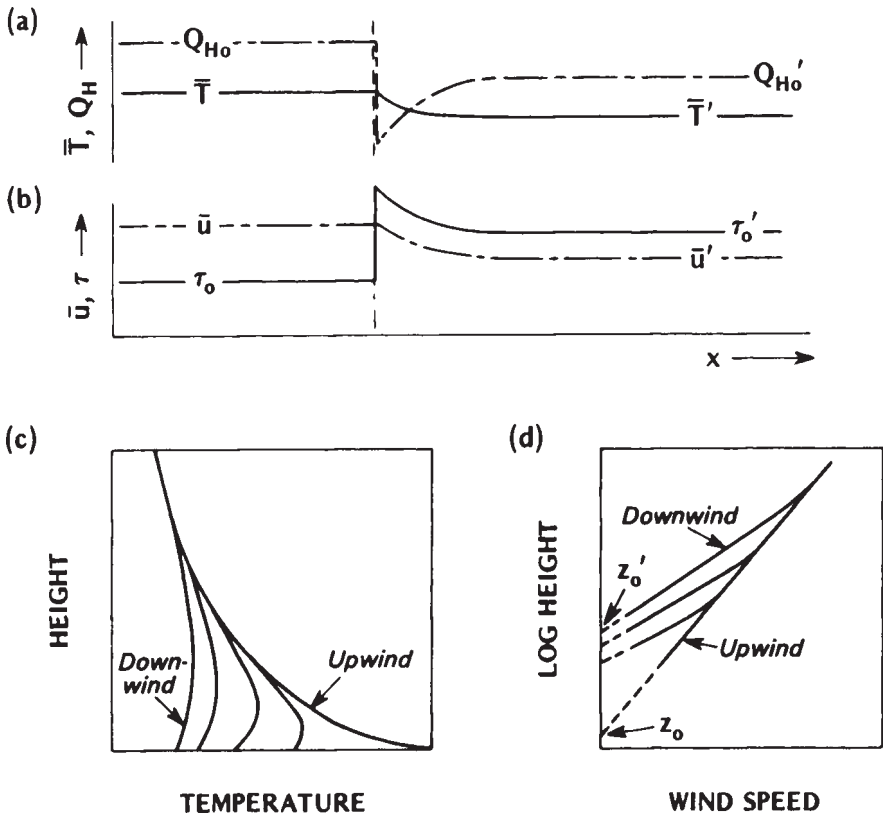
Figure 5.3 (a) Adjustment of surface sensible heat flux (Q_{H_i}) and mean air temperature ($\bar{T}$) as air passes from a hot to a cooler surface, (b) Change in surface shearing stress (t_0) and mean wind speed (*u*) as air flows from a smooth to a rougher surface. Associated modification of the vertical profiles of (c) air temperature, and (d) wind speed at different distances downwind of the leading edge.

directed *towards* the surface. The heat involved in this flow will be drawn from the advecting hot air and therefore contributes to its cooling (Figure 5.3a) until a new equilibrium temperature is established. The greater roughness of the vegetation will exert a greater drag on the air. This increases the surface shearing stress and decreases the mean wind speed (Figure 5.3b). The wind profile in the upwind region (Figure 5.3d) is logarithmic, and its extrapolation would intersect the height axis at a small value of z_0 (see p. 57). Downwind of the leading edge the profiles have a 'kink' where the steeper slope of the new profile intersects that of the upwind profile. The point of intersection becomes higher as the boundary-layer adjustment deepens downwind. The greater slope reflects the increased shearing, and extrapolates to a much larger roughness length, z_0' (Figure 5.3d).

In reality for a case such as we have been discussing it is not possible to separate entirely the changes in energy, mass and momentum. For example the momentum changes will increase the turbulent diffusivities $(K's)$ over the rougher surface, and hence enhance Q_E and Q_H even if the vapour and temperature gradients did not change.

Leading-edge effects occur wherever there is a marked discontinuity in surface properties. Figure 5.4 shows a surface temperature cross-section obtained from a radiation thermometer mounted on an aircraft. The instrument senses L? and this can be related to surface temperature from equation 1.4 if the emissivity of the radiating surfaces is known (p. 361). This midday transect across the prairies shows sharp changes in temperature (up to 35 Celsius degrees) due to the different climatic properties of cultivated/uncultivated, dry/irrigated farm land, and water bodies. The vertical structure shows the development of a series of boundary layers, some warmer and some cooler than the bulk air temperature. At the upwind edge of each new surface an internal boundary layer forms, and hence the structures appear as hot or cool 'plumes'. The heated plumes being unstable
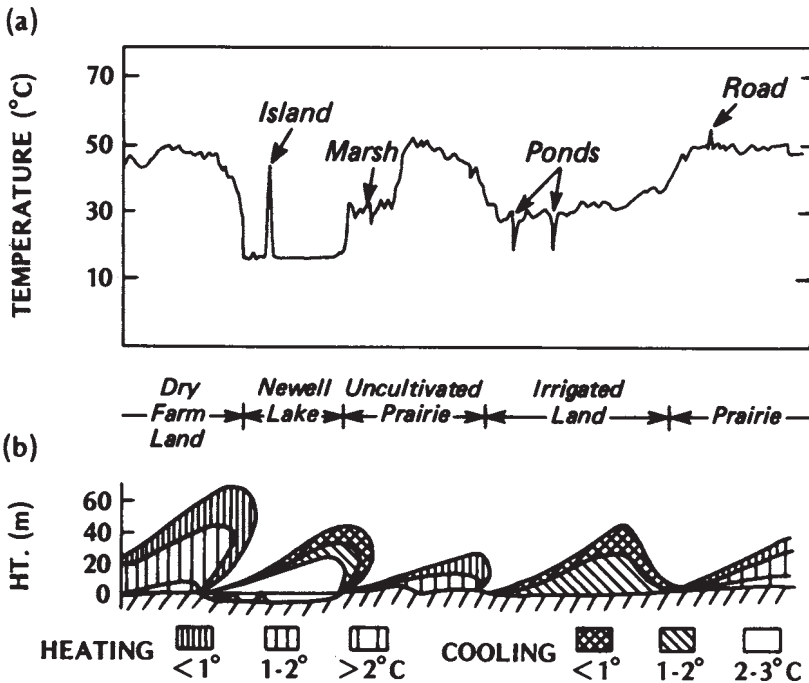

Figure 5.4 (a) Horizontal profile of surface radiation temperature, and (b) hot and cold 'plumes' over a diverse prairie landscape. Based on aircraft observations on the afternoon of 6 August 1968 near Brooks, Alberta (after Holmes, 1969).

have more vigorous vertical development than those from the cooler, more stable lake or irrigated-land. The former were found up to 1000 m, the latter never above 60 m.

There are two types of fog which illustrate the effect of advection of air across water of a very different temperature. Paradoxically one occurs with warm air flowing over cold water, the other with cold air over warm water. Near coastlines winds or ocean currents can cause cold water to well up to the surface from below. Air flowing towards the land across the warmer surface waters offshore encounters the leading edge of this band of cold water along the coastline and the lowest air layers are cooled. If air temperatures are depressed to the dew-point a band of *cold-water advection fog* is formed. Another leading edge is crossed at the coastline and the lowest layer becomes re-heated over the warmer land surface. The fog therefore thins out from below as it travels inland and evaporates.

On the other hand *warm-water advection fog* occurs when very cold air is transported across a much warmer water body. The saturation vapour content at the water surface therefore exceeds the vapour content of the air, whether it is saturated or not. The warmer, moister surface air is unstable and convects moisture easily up into the cooler air. Some of the super-saturated mixture then condenses to give a fog which visually appears like rising steam (the same effect is evident with exhaled breath on a cold day, or when hot water is run into a bath in a cool room). These conditions can occur over arctic oceans (where it is called arctic sea 'smoke'), or over open bodies of water in otherwise cold continental climates, and over some industrial cooling ponds. It can also be seen over lakes on summer or autumn mornings, especially if during the night cold air has drained down onto the lake from the surrounding hills.

(iii) 'Oasis effect'

Due to evaporation cooling, an isolated moisture source always finds itself cooler than its surroundings in an otherwise rather arid region. The desert oasis is the most obvious example of this situation. Table 5.1 shows the energy and water balances of oases in comparison with their surrounding terrain. The semi-desert area evaporates all of its precipitation leaving virtually nothing for runoff. Even so this consumes only a small proportion of the available radiant energy because precipitation is so limited. The surplus heat is therefore dissipated as sensible heat to warm the air, resulting in a large Bowen ratio *(ß)*.

In the oases on the other hand, the free availability of water permits evaporation to exceed precipitation by one order of magnitude, and the energy necessary to accomplish this is more than that supplied by radiation (i.e. Q_E is greater than Q^*). This apparently anomalous situation is explained by the fact that the *atmosphere* supplies sensible heat to the surface because

Table 5.1 Annual energy and water balances of Tunisian Oases (after Flohn, 1971).

Surface type	Area (km^2)	Albedo α	Q^*	Q_H	Q_E	β	Q_E/Q^*	E	p
			(MJ m^{-2} day^{-1})					(mm yr^{-1})	
Semi-desert	35,000	0·20	6·9	5·8	1·0	5·8	0·14	150	150
Oases (av.)	150	0·15	8·6	−3·1	11·8	−0·26	1·37	1680[†]	150

[†] To support this evaporation rate the precipitation supply is supplemented by irrigation from artesian wells.

Note: On an annual basis $Q_G \simeq 0$

the oasis is cooler than the regional air in which it is embedded. Therefore there is a continual air-to-oasis inversion temperature gradient driving a downward directed heat flux, and the process is aided by air mass subsidence over the oasis. (Note that the reversal of Q_H gives the oasis a negative Bowen ratio.)

In this example the ratio Q_E/Q^*=1·37. In an extreme case the 'oasis effect' has been observed to produce a ratio of Q_E/Q^*=2·5 for a shorter period over an irrigated field of cotton (Lemon *et al.*, 1957). The irrigated field of alfalfa near Phoenix, Arizona considered previously in relation to Figure 4.16, also exhibits the 'oasis-effect'. Figure 5.5 shows the average daily energy balance components in June following the irrigation in late May. For the first half of June an 'oasis effect' is clearly evident; evapotranspiration exceeds the net radiation, and Q_H is directed towards the crop. During this period the average Bowen ratio is about -0·25, and the ratio Q_E/Q^* is approximately 1·5. However, by the middle of June soil moisture starts to become restricted, the surface resistance (r_c) increases, and evaporation rates decrease. Since Q^* remains relatively constant this requires an adjustment by Q_H. By 25 June the Bowen ratio is +1·0, and Q_E/Q^* is about 0·5. In the absence of further irrigation or precipitation the energy balance would return to a semi-arid type.

Many other 'oasis-effect' advective situations can be envisaged. In each of the following examples a cool, moist surface is dominated by larger-scale warmer, drier surroundings: a lake in an area with a dry summer climate; a glacier in a mountain valley; an isolated snow patch; an urban park; an isolated tree in a street or on open, bare ground. In each case we may expect evaporation to proceed at an increased rate compared with that from an extensive area of the same composition, and it is quite possible that the energy required to accomplish this will exceed the local radiative surplus.
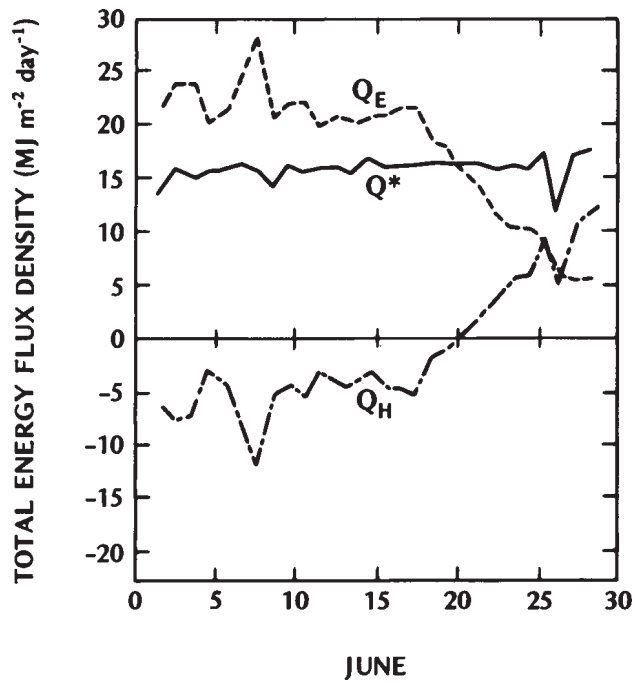
Figure 5.5 Average daily energy balance of an alfalfa crop in June 1964 near Phoenix, Arizona (33°N). The crop was irrigated by flooding in late May and this was followed by drought throughout June (see Figure 4.16) (after van Bavel, 1967).